AIP Advances

Numerical estimation on free electrons generated by shielded radioactive materials under various gaseous environments

D. S. Kim, W. S. Lee, J. H. So, and E. M. Choi

Citation: AIP Advances **3**, 062109 (2013); doi: 10.1063/1.4811177
View online: http://dx.doi.org/10.1063/1.4811177
View Table of Contents: http://aipadvances.aip.org/resource/1/AAIDBI/v3/i6
Published by the AIP Publishing LLC.

AIP ADVANCES **3**, 062109 (2013)

Numerical estimation on free electrons generated by shielded radioactive materials under various gaseous environments

D. S. Kim,[1] W. S. Lee,[2] J. H. So,[2] and E. M. Choi[1,3,a]
[1]*Department of Physics, Ulsan National Institute of Science and Technology (UNIST), Ulsan 689-798, Republic of Korea*
[2]*Agency for Defence Development (ADD), Daejeon 305-152, Republic of Korea*
[3]*School of Electrical and Computer Engineering, Ulsan National Institute of Science and Technology (UNIST), Ulsan 689-798, Republic of Korea*

(Received 27 December 2012; accepted 31 May 2013; published online 7 June 2013)

We report simulation results on generation of free electrons due to the presence of radioactive materials under controlled pressure and gases using a general Monte Carlo transport code (MCNPX). A radioactive material decays to lower atomic number, simultaneously producing high energy gamma rays that can generate free electrons via various scattering mechanisms. This paper shows detailed simulation works for answering how many free electrons can be generated under the existence of shielded radioactive materials as a function of pressure and types of gases. [http://dx.doi.org/10.1063/1.4811177]

I. INTRODUCTION

Increasing threat of nuclear material related incidents motivates researchers to devise a remote sensing scheme of radioactive material. However, sensing presence of radioactive materials in a long distance away is extremely challenging task whereas detecting it in near sight has been commonly done for various purposes in many fields.

Recent study by Nusinovich *et al*. in Univ. Maryland shows the possibility for detecting a radioactive material remotely by utilizing high power millimeter/THz wave sources for generating plasma breakdown.[1,2] High energy gamma photons (>a few MeV) are emitted by radioactive decay process. For example, in the decay process, Co60 emits two energy gamma rays, 1.17 MeV and 1.33 MeV. These high energy gamma photons can penetrate through a metal shield, which can be utilized as an indirect signal for sensing existence of radioactive material under concealed environment. The high energy gamma rays from radioactive material generate free electrons at background via Compton scattering. Nusinovich *et al*. proposed to use a high power THz gyrotron as a probing tool for radioactive material via generated free electrons. Focused high power THz beam at a target distance can enhance avalanche plasma breakdown when there are enough free electrons in background as schematically shown in Fig. 1. Plasma breakdown at ambient or controlled pressurized environment has been observed using millimeter wave sources and lasers.[3–5] Plasma filaments observed in air breakdown using a millimeter wave source have drawn interests from many researchers and have been under investigation theoretically to resolve the peculiar structure.[6–8] The possibility of air plasma breakdown using millimeter wave at MW power level opens a way for the realization of plasma breakdown at THz at much lower power.

The proposed technique to use a high power THz source is thought to be a breakthrough for remote detection of concealed radioactive material which has not been possible up to now. Basic research regarding this scheme has been undertaken including estimates for requirements and the

[a]Corresponding author: emchoi@unist.ac.kr

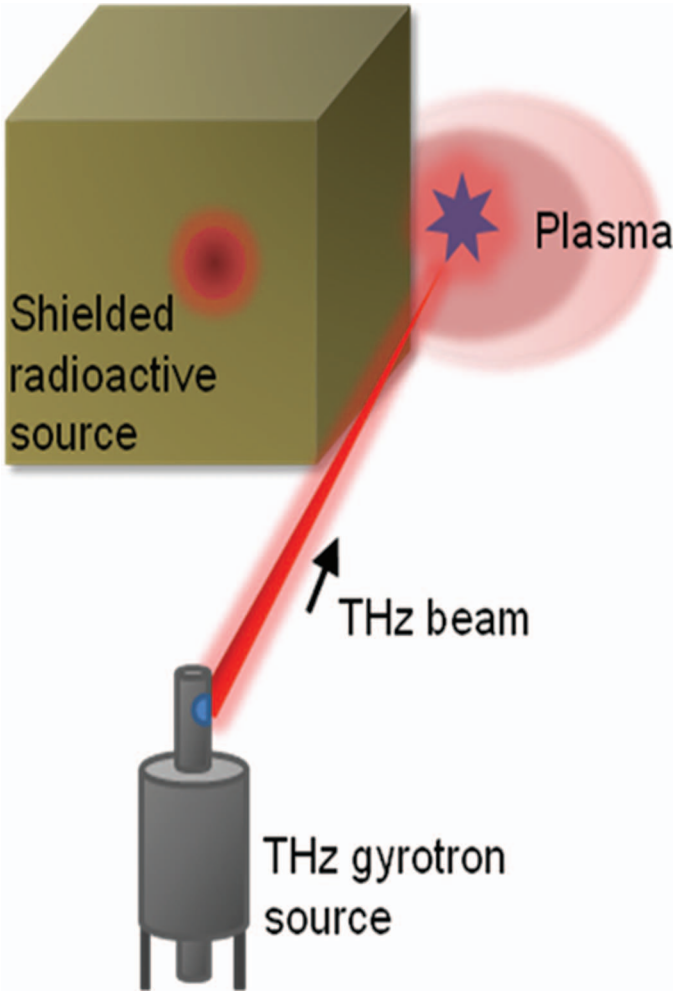

FIG. 1. Conceptual schematic of detecting radioactive material by a high power THz source: Plasma formed by focused THz beam due to free electrons from shielded radioactive source.

experimental demonstrations in order to achieve initial breakdown at a distance away in some groups.[9,10]

The optimal power density as well as frequency for efficient breakdown at atmospheric pressure has been also suggested in the recent paper.[2] Estimates for the number of free electrons generated by a radioactive material which is under shielded environment are critical for implementing the scheme. The recent study by Dimant *et al*. analyzed of the free electron production rate at distance from a radiation source and showed an excellent agreement between the analytic solution from the Klein-Nishina scattering theory and the numerical solution from MCNPX.[11] In this study, Dimant *et al*. showed an important finding that the free electron production rate decays slower when the total free-electron production rate includes the scattered-photon contribution than that of when only primary photons are considered.[11] Nusinovich *et al*. quantitatively analyzed the detectable mass of radioactive material as the function of the distance and the THz power level and pulse duration.[12]

The quantitative estimates for the free electrons under various environmental conditions for the proof-of-principle are very important for analyzing the experimental data in the laboratory. In this paper, we investigate quantitative analysis of the experimental situation to estimate the free electron production rate on the material property of a container, gas pressure in the container, and the thickness of the container which are all control parameters in the proof-of-principle experiment.

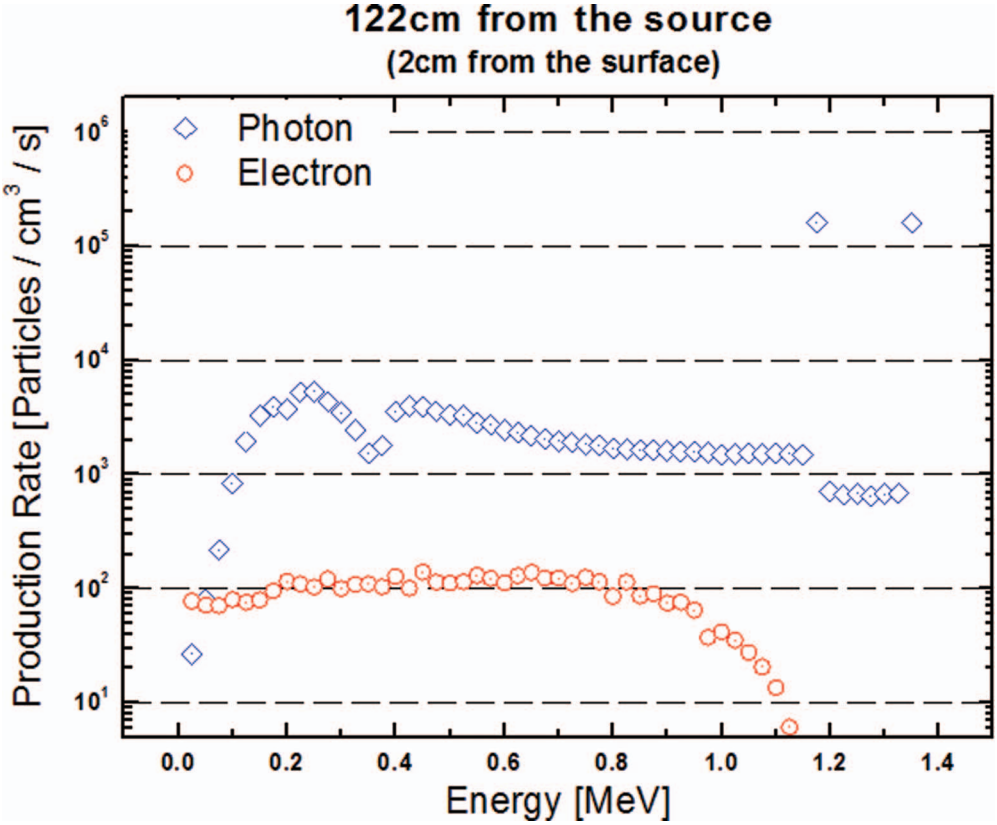

FIG. 2. The production rate of electrons and gamma photons as a function of energy. The data was taken at 2 cm away from the container outer surface where the source is present at 120 cm inside of the container.

II. SIMULATION SETUP

The Monte Carlo N-Particle Code (MCNPX) has been used for the simulation of this work.[13] The MCNPX has been and is being widely used for simulating the radiation transport of radioactive source via various physical interacting processes and benchmarked against other particle transport codes and experiments.[13–16] In the simulation, we have set the mode for photon and electron transport which deals with electron/photon production by electron/photon transport. Electrons are produced from various interactions such as the Compton interaction, Rayleigh scattering, the photoelectric interaction, and electron positron pair production, that are all included in the data library for energy level of our interest (a few keV to tens of MeV). We have positioned a 1Ci Co60 source inside a container whose thickness and material composition are varied in the simulation. For experimental tests to demonstrate the proposed detecting scheme, one need control gases inside the container which is also a parameter in the simulation.

III. RESULTS

Fig. 2 shows the result of gamma and electron production rate as a function of energy. The thickness of the container wall is 0.5 cm, and the diagnostics point is set at 2 cm away from the container surface where 1Ci of Co60 radioactive source is contained 120 cm away from the container inner surface. The container is composed of stainless steel whose material composite is Cr 19 %, Ni 9.5 %, Mn 2 %, and Fe 69.5 %. As shown in Fig. 2, the production rate of electron at 2 cm away from the container surface is much more than that of under normal environment where there exists no radioactive material. At atmospheric pressure, around 20 free electrons /cm^3 s are known to be present occasionally.[1]

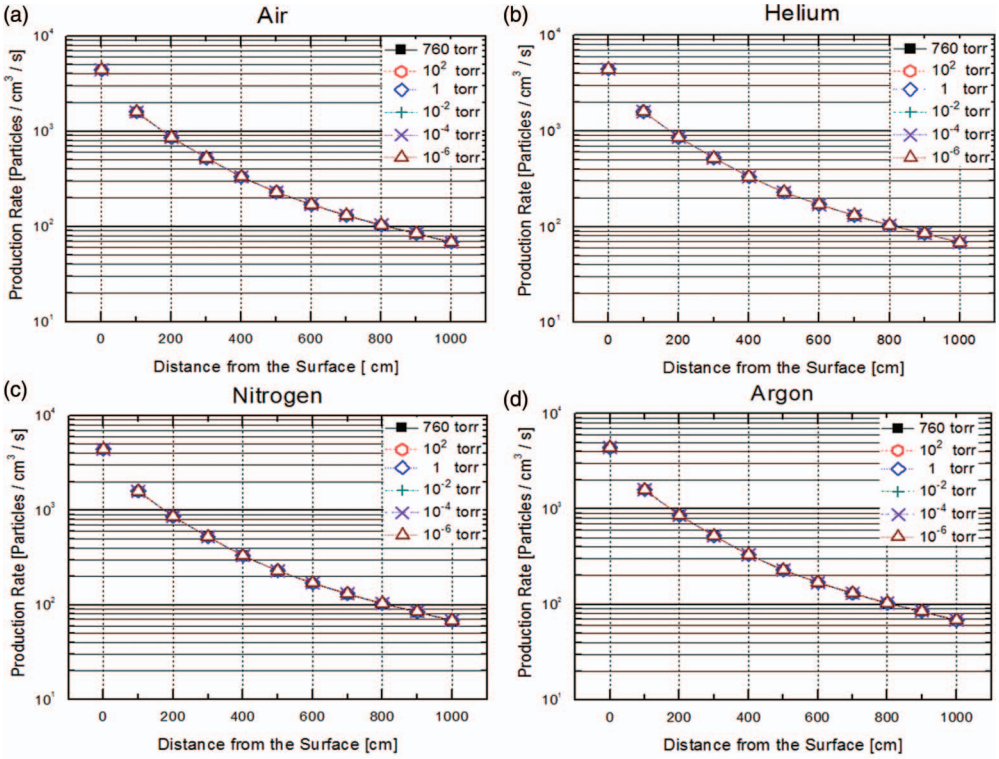

FIG. 3. The electron production rate as a function of distance from the surface when the container is filled with (a) Air, (b) Helium, (c) Nitrogen, and (d) Argon inside the container. The container is set to be 0.5 cm thick stainless steel and the pressure in the container is varied.

Fig. 3 shows the simulation results of the electron production rate as a function of distance from the container surface. The material composite and the thickness of the container are fixed to be stainless steel and 0.5 cm, respectively. Different gaseous environment inside the container was considered in the simulation to represent experimental situation. Also, the pressure inside the container was varied from 760 Torr down to 1 μTorr. According to Fig. 3, the number of free electrons generated by the concealed radioactive material does not depend on the type of gases and the pressure of the gas inside the container. The number of particle is around 4000 electrons per cubic centimeter per second in vicinity of the container surface, which is 2 orders of magnitude greater compared to the case of no radioactive material. Away from the container, the number decreases exponentially as expected. It is noteworthy that the electron production rate does not depend on the pressure inside the container at all when the distance from the surface is more than 1 m away. Also, gas type in the container does not affect the production rate of electron generated outside the container wall.

Fig. 4 shows the simulation results of the electron production rate and the electron energy spectrum as a function of distance from the surface. Stainless steel, lead, and aluminum are used in the simulation for the material of the container. The gas and the pressure inside of the container are fixed to be air and 760 Torr, respectively. The thickness of the container is varied to be from 0.01 mm to 1 cm. For the stainless steel container as shown in Fig. 4(a), the production rate increases when the thickness of the container increases up to 5 mm compared to the case of no container, and starts to decrease when the thickness is greater than 5 mm. The same result can be found in the lead container case as shown in Fig. 4(b), although the extent of the increasing number of free electrons as the container thickness increases diminishes up to the 10 μm due to the high density of the material composite of the lead material. For the aluminum container in Fig. 4(c), the electron production rate increases up to 2 cm of the thickness compared to no container, where the maximum number of free electrons occurs at 3 mm thickness. In other words, the generated free electrons are more when the

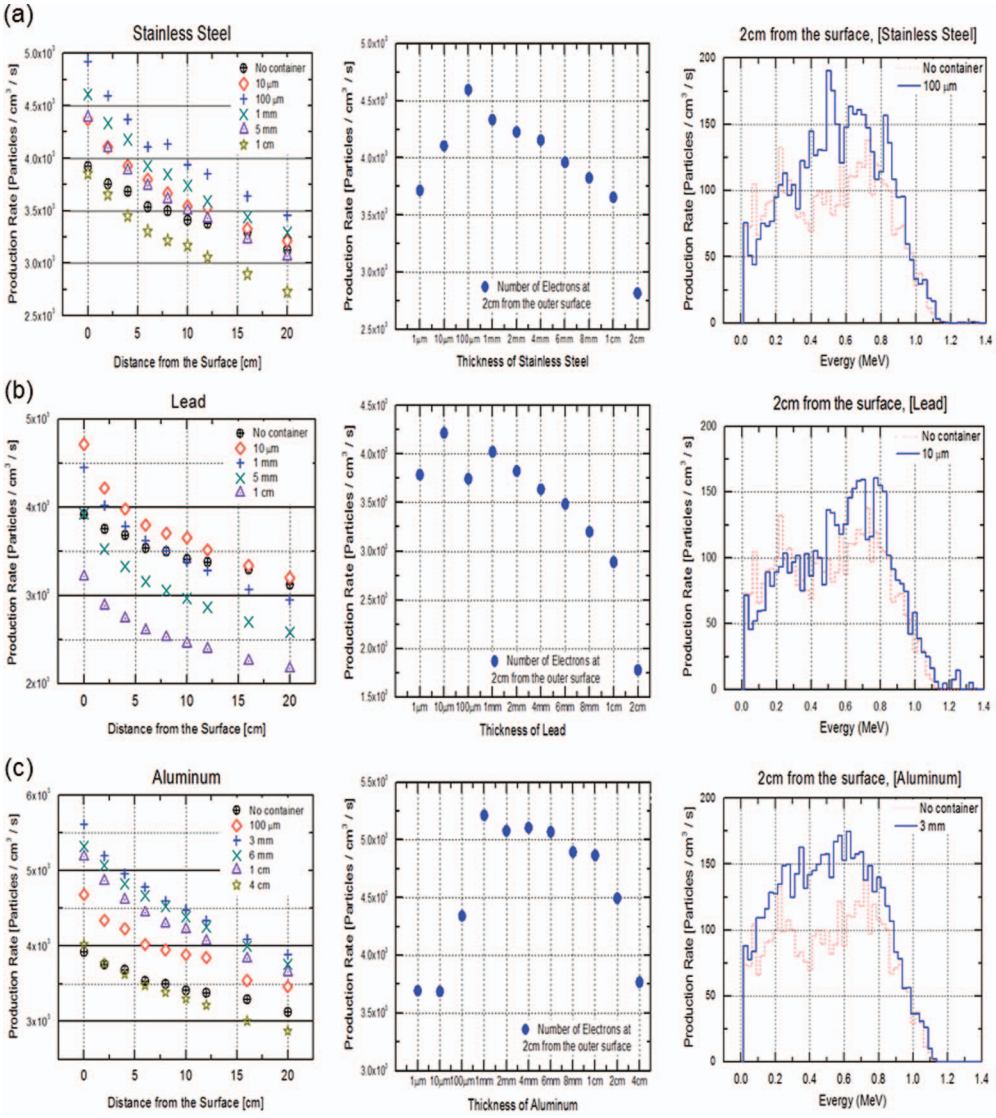

FIG. 4. The electron production rate and the electron energy spectrum as a function of distance: The thickness of the container is varying at fixed pressure of 760 Torr inside the container. The material property is varied in the simulation: (a) Stainless steel, (b) Lead, and (c) Aluminum.

radioactive material is shielded with metal container. The electron production rate as a function of energy dramatically shows that when the radioactive material is inside the container, there are more electrons generated outside of the container compared to the case of no shielding by the container. This behavior on effect of shielding has been also found in the recent study by Dimant *et al.*, with observation of pronounced energy distribution in a close proximity to the source in the presence of shielding material.[11] These interesting findings of increasing the production rate of electron with increasing container thickness can be interpreted as follows. While the high energy gamma photons are penetrating out of the container, the interactions between the gamma photons and the material inside the container give rise to the strong Compton interaction up to some thickness, therefore, in vicinity of the container (less than 20 cm away from the container surface), more electrons can be generated in the energy scale between ∼100 keV and ∼1 MeV. However, as the thickness of the container increases further, the net cross section of the scattering inside the container material diminishes which is essentially reducing the energy of the gamma photons.

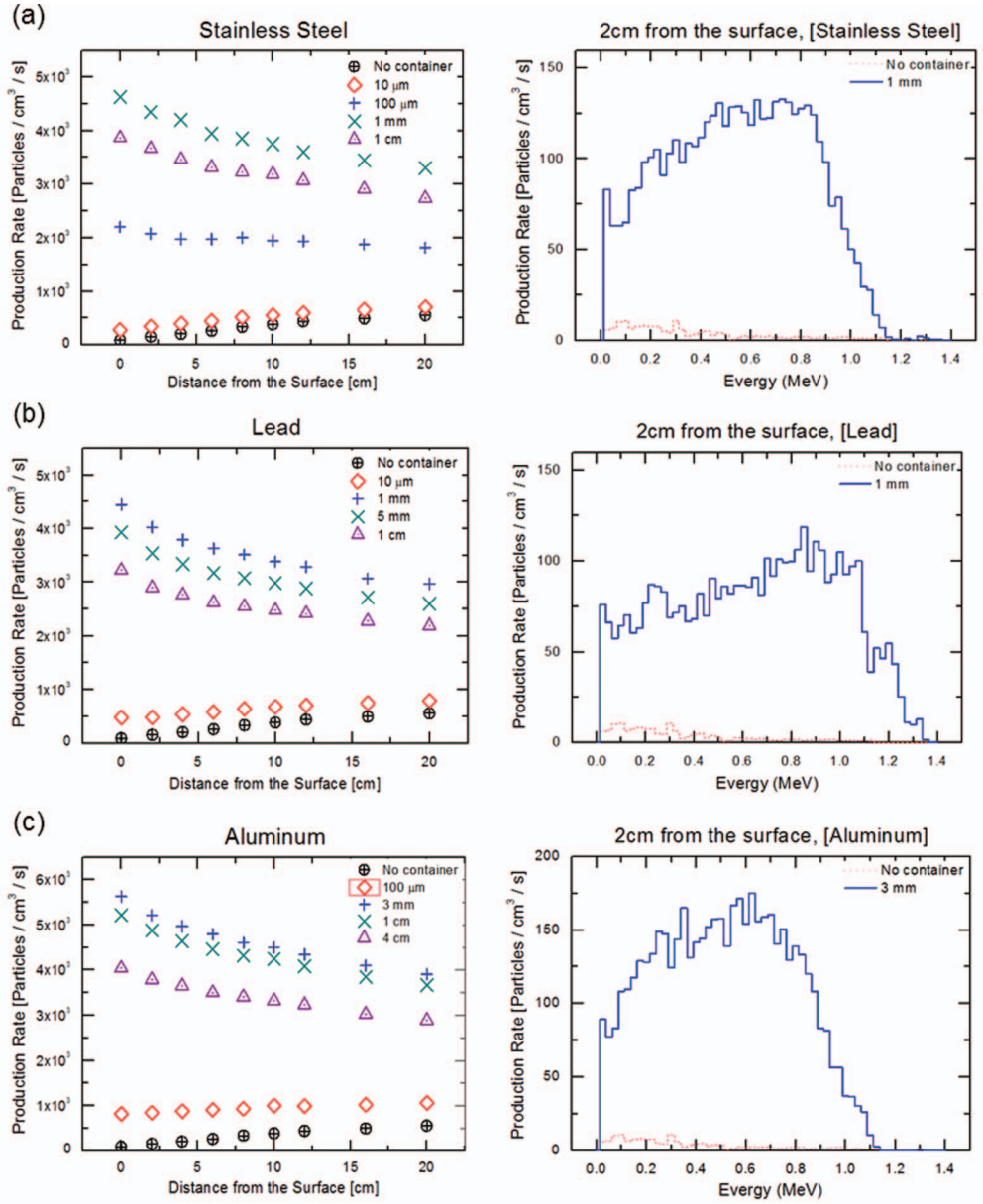

FIG. 5. The production rate of electron and the electron energy spectrum as a function of distance: The thickness of the container is varying at fixed pressure of 1 mTorr inside the container. The material property is varied in the simulation: (a) Stainless steel, (b) Lead, and (c) Aluminum.

Fig. 5 shows the result of the same simulation as Fig. 4, but the pressure and the gas inside the container were changed to 1 mTorr and Helium, respectively. The electron production rate peaks at 1mm thickness of the stainless steel container compared to Fig. 4(a). The electron production rate when the thickness of the lead container is 1 cm increases by order of magnitude compared to no container case as shown in Fig. 5(b). The aluminum container case gives the same result that the production rate of electron increases by order of magnitude greater for the 4 cm thickness case compared to no container case when the pressure and the content of the gas are 1 mTorr and Helium in Fig. 5(c). The electron energy spectrum is compared for the case of with and without the radioactive material inside container at specified simulation condition, and significant difference in energy spectrum is shown. When the pressure in the container is low, the gamma photon interacts

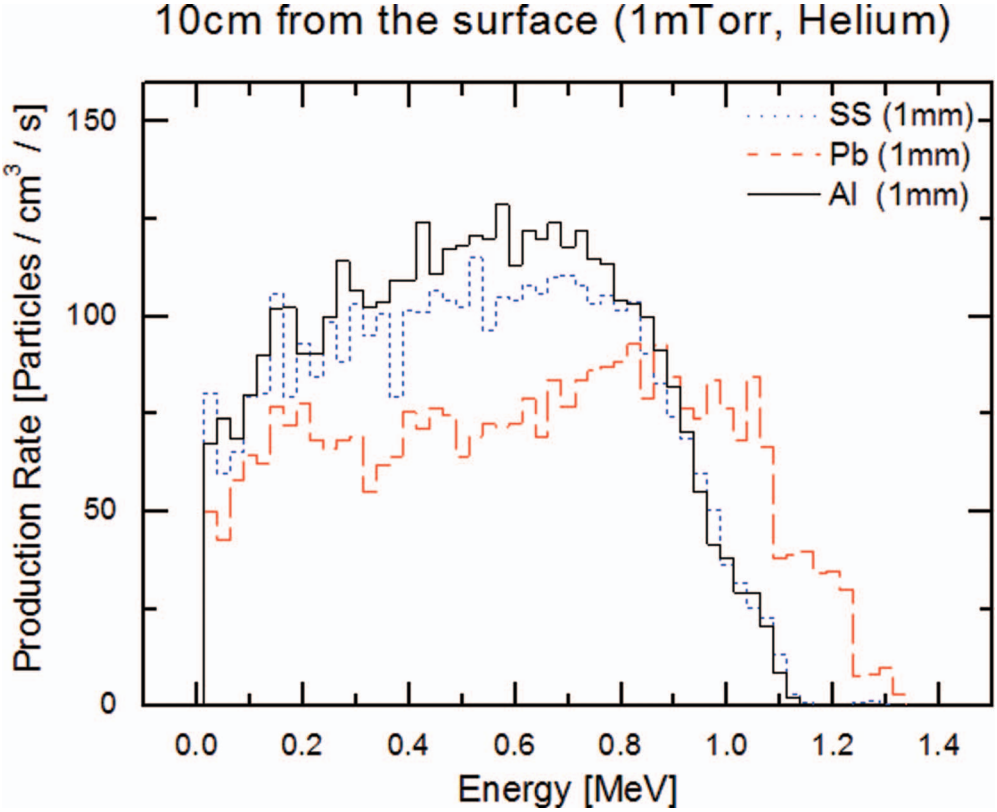

FIG. 6. The electron energy spectrum at different container material at fixed thickness.

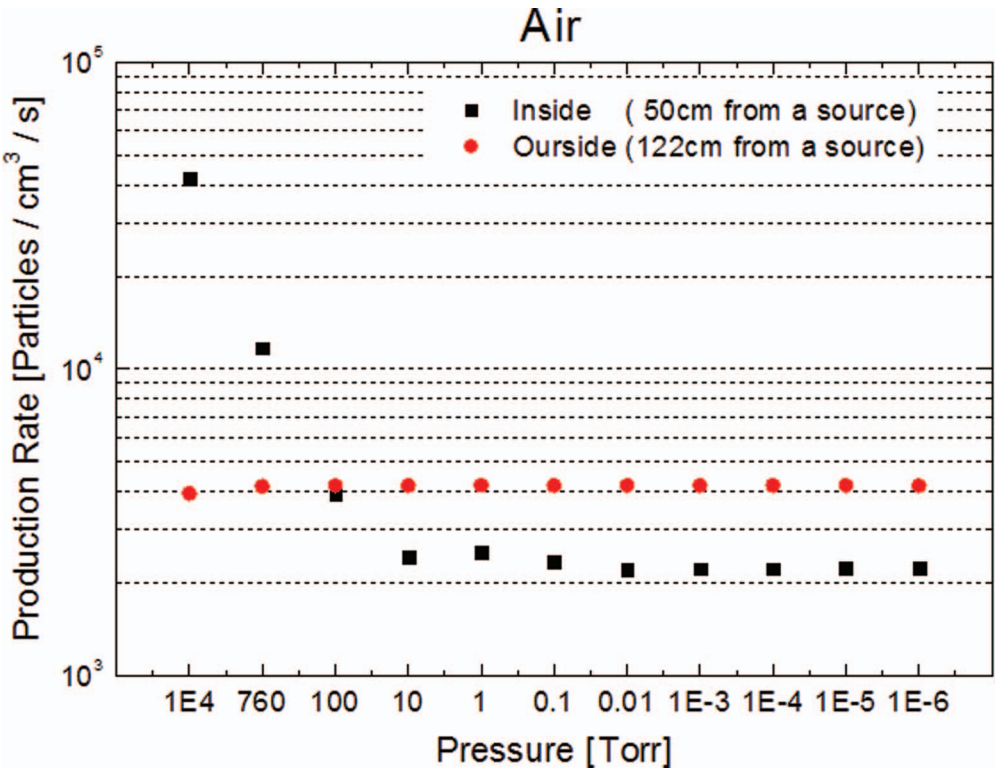

FIG. 7. The production rate as a function of pressure of air in the container for the two different location from the source. The thickness of the stainless steel container is fixed to be 0.5 cm.

TABLE I. The collisions of air molecules and gamma-rays, produced by 1Ci of Co60, at 50 cm from the radioactive source as function of pressure.

Pressure (Torr)	Collision of particles (Atom fraction rate)			
	N_2 (0.784)	O_2 (0.211)	Ar (0.00467)	C (0.00015)
10^4	11236	3528	225	1
760	851	264	15	0
1	2	0	0	0
10^{-6}	0	0	0	0

with gases less, which results in higher gamma photon energy, that may result in more scattering events inside the container material. This implies that one might be able to observe the difference in the breakdown event when the radioactive material is concealed by lead and without lead at 1 mTorr pressure of Helium in the proof-of-principle experiment.

Fig. 6 shows the result of the electron energy spectrum measured 10 cm away from the surface when the pressure and the gas in the container are fixed to be 1 mTorr and Helium, respectively. The total number of electrons is greater in the case of the aluminum container than that of the lead container at fixed thickness.

Fig. 7 shows the simulation result of the production rate as a function of pressure in the container when the measurement was done at 50 cm away from the source inside the container and 2 cm away from the container outer surface. As shown in Fig. 7, as the pressure in the container decreases, the production rate decreases when measured inside the container, while the production rate does not vary as the pressure varies when measured outside the container. Increasing the production rate with increasing pressure is attributed to increased collision events, and the number of collision events is checked at various pressures as summarized in Table I.

It is shown that as the pressure of atmosphere continues to increase up to 10^4 Torr, the number of collisions between the air molecules and gamma-ray photons increases steadily as shown Table I. Below 760 Torr, collisions do not occur under the same condition. From the result, it is noticeable that the inner pressure of the container box under 760 Torr has negligible effect on the amount of free electrons generated out of the container at a fixed thickness.

IV. CONCLUSIONS

We have conducted extensive MCNPX simulation work for estimating the electron production rate generated by high energy gamma photons to demonstrate the scheme for remote detection of radioactive material. The scheme is based on the existence of abundant free electrons to make plasma breakdown. From the simulation work, we have quantitatively estimated the electron production rate generated by photon/electron interactions and their transports. In order to demonstrate the laboratory experimental condition, we have simulated various gaseous conditions with choosing versatile container materials and thickness under varying pressure and gas contents in the container. The electron production rate present out of the container does not depend on the pressure or gas content in the container box. However, it is highly dependent upon the thickness of the metal container. The production of free electrons increases as the container thickens unlike one's expectation. Around ~4000 of electrons per cubic centimeters per second are present in most circumstances when the detecting location is more than 1 m away from the source and this number is significantly increased value compared to ~20 electrons per cubic centimeters per second being without radioactive material nearby. The work that we have presented in this paper will give insight for performing laboratory experiments for the future research.

ACKNOWLEDGMENTS

We wish to thank Mr. Chul-Woo Lee at Korea Atomic Energy Research Institute (KAERI) and Prof. Yonghee Kim at Korea Advanced Institute of Science and Technology (KAIST) for

helpful discussions of MCNPX simulation. We acknowledge financial support by Contract No. UD100039GD and No. UD100038GD by Agency for Defense Development.

[1] G. S. Nusinovich, R. Pu, T. M. Antonsen, O. V. Sinitsyn, J. Rodgers, A. Mohamed, J. Silverman, M. Al-Sheikhly, Y. S. Dimant, and G. M. Milikh, "Development of THz-range gyrotrons for detection of concealed radioactive materials," Journal of Infrared, Millimeter and THz Waves **32**, 380–402 (2011).
[2] V. L. Granatstein and G. S. Nusinovich, "Detecting excess ionizing radiation by electromagnetic breakdown of air," Journal of Applied Physics **108**, 063304 (2010).
[3] Y. Hidaka, E. M. Choi, I. Mastovsky, M. A. Shapiro, J. R. Sirigiri, and R. J. Temkin, "Observation of large arrays of plasma filaments in air breakdown by 1.5 MW 110 GHz gyrotron pulses," Physical Review Letters **100**, 035003 (2008).
[4] Z. Zhang, M. N. Shneider, and R. B. Miles, "Microwave diagnostics of laser-induced avalanche ionization in air," Journal of Applied Physics **100**, 074912 (2006).
[5] X. Xie, J. Dai, and X. C. Zhang, "Coherent control of THz wave generation in ambient air," Physical Review Letters **96**, 075005 (2006).
[6] A. Cook, M. Shapiro, and R. Temkin, "Pressure dependence of plasma structure in microwave gas breakdown at 110 GHz," Applied Physics Letters **97**, 011504 (2010).
[7] J. T. Krile and A. A. Neuber, "Modeling statistical variations in high power microwave breakdown," Applied Physics Letters **98**, 211502 (2011).
[8] J. Foster, H. Krompholz, and A. Neuber, "Investigation of the delay time distribution of high power microwave surface flashover," Physics of Plasmas **18**, 013502 (2011).
[9] C. A. Romero-Talamas, "Experimental program to test a high-power, 670 GHz gyrotron, and its applicability to the remote detection of concealed radioactive materials," *International Vacuum Electronics Conference (IVEC) 2012*, Monterey, California, (2012).
[10] N. Kumar, U. Singh, A. Kumar, and A. K. Sinha, "A feasibility study of beam-wave interaction in 670 GHz gyrotron for radioactive material detection application," Japanese Journal of Applied Physics **50**(7), 076705 (2012).
[11] Y. S. Dimant, G. S. Nusinovich, P. Sprangle, J. Penano, C. A. Romero-Talamas, and V. L. Granatstein, "Propagation of gamma rays and production of free electrons in air," Journal of Applied Physics **112**, 083303 (2012).
[12] G. S. Nusinovich, P. Sprangle, V. E. Semenov, D. S. Dorozhkina, and M. Yu. Glyavin, "On the sensitivity of terahertz gyrotron based systems for remote detection of concealed radioactive materials," Journal of Applied Physics **111**, 124912 (2012).
[13] http://mcnpx.lanl.gov/.
[14] R. Jeraj, P. J. Keall, and P. M. Ostwald, "Comparisons between MCNP, EGS4 and experiment for clinical electron beams," Physics in Medicine and Biology **44**, 705–717 (1999).
[15] T. E. Valentine and J. T. Mihalczo, "MCNP-DSP: A neutron and gamma ray Monte carlo calculation of source-driven noise-measured parameters," Annals of Nuclear Energy **23**(16), 1271–1287 (1996).
[16] R. A. Forster, R. C. Little, J. F. Briesmeister, and J. S. Hendricks, "MCNP capabilities for nuclear well logging calculations," IEEE Transactions on Nuclear Science **37**(3), 1378–1385 (1990).